



# Inside spherically symmetric black holes or how a uniformly accelerated particle may slow down

Andrzej Radosz<sup>1</sup>, Pawel Gusin<sup>2</sup>, Andy T. Augousti<sup>3,a</sup> , Filip Formalik<sup>4</sup>

<sup>1</sup> Department of Quantum Technologies, Wrocław University of Science and Technology, Wrocław, Poland

<sup>2</sup> Faculty of Technology and Computer Science, Wrocław University of Science and Technology, Wrocław, Poland

<sup>3</sup> Faculty of Science, Engineering and Computing, Kingston University London, London, UK

<sup>4</sup> Faculty of Chemistry, Wrocław University of Science and Technology, Wrocław, Poland

Received: 31 May 2019 / Accepted: 3 October 2019 / Published online: 24 October 2019  
© The Author(s) 2019

**Abstract** Three types of phenomena occurring on both sides of the event horizon of spherically symmetric black holes are analyzed and discussed here. These phenomena are: a light ray orbiting a photon sphere and its analogue, the motion of a uniformly accelerated massive particle and a generalized Doppler effect. The results illustrate how the anisotropic dynamics of the interior of black holes, distinct in the cases both with and without an additional internal horizon, affect non-quantum behaviour.

## 1 Introduction

Recent studies of black holes have brought a range of interesting results. The most significant of these are those related to the information problem [1]. The idea presented recently [2] that black holes do have hair contradicted a former fundamental assumption that black holes don't have hair. The claim that the volume of a black hole may be infinite, derived in different ways in Refs. [3] and [4], contributed to the information problem – this actually implies that an arbitrarily large amount of information may be stored there. The scenario of the evolution of the information contained in the interior of a black hole (BH) was presented by Braunstein et al. [5].

The interior of a BH may be described with a so-called “river model” as shown in [6] (see also [7]). A different perspective has appeared from more recent studies [8, 9]. Hamilton et al. [10] considered the question of vision inside the horizon of a Schwarzschild BH. In Ref. [11] the evolution of a light ray trapped at one of the two BH horizons was investigated – it led to a redshift on the outer event horizon and a blueshift on the inner horizon. It is well-known that spacetimes that are static outside the horizon of BHs turn out to be

dynamic inside the (outer) horizon. Such a dynamic interior of a BH may be viewed as a cosmological model [12].

In this paper, we will analyse selected (non-quantum) phenomena illustrating the properties of the interior of a spherically symmetric BH, in Schwarzschild (S), Reissner–Nordström (RN) and Anti-de Sitter AdS spacetimes. Our considerations are illuminated by a comparison of the regions outside and inside the horizon (S, AdS) or between horizons (RN). We will discuss the following questions.

Outside the horizon there exists a so-called photon sphere; we will prove the existence of its analogue inside the horizon. A light ray may, in principle circulate on a photon sphere so in a sense the deflection angle in a strong gravitational field would be arbitrary large. The revolution angle of a light ray following an orbit belonging to a photon sphere analogue inside the horizon should be finite. So, not surprisingly it turns out to be finite. Rather surprising, though, is its value,  $\pi$  (for S and RN spacetimes) and the possible deeper meaning and interpretation of this outcome.

The problem of a uniformly accelerated test particle will be solved outside and inside the horizon, as well as between horizons in the RN case. In Minkowski spacetime, such hyperbolic motion results in Unruh radiation. We show here that outside the BH, uniformly accelerated (radial) motion is described in terms of equations similar to those representing motion in Minkowski spacetime. Inside the horizon of a Schwarzschild spacetime one comes across a counter-intuitive outcome: the speed of such a test particle initially grows but then reaches a maximal value and finally decreases to zero (as clarified further below the meaning of speed needs to be specified inside the horizon). In the case of a BH possessing an internal horizon, (the RN case) the speed of a uniformly accelerated particle turns out to behave in a more complex manner but in accordance, as explained later, with the dynamical properties of its interior.

<sup>a</sup> e-mail: [augousti@kingston.ac.uk](mailto:augousti@kingston.ac.uk)

The Doppler shift of electromagnetic signals exchanged between resting/co-moving observers occupying fixed positions outside and inside (between) the horizon(s) will be investigated - the outcomes will reflect the dynamic properties of the interior, distinct for S and AdS spacetimes on the one hand and RN spacetime on the other.

This paper is organized as follows. In Sect. 2 we formulate the framework of our considerations: a general form of a line element for spherically symmetric spacetimes is given and two kinds of observers, resting outside and co-moving inside the horizon, are introduced. In the following sections we consider the problems of: the value of the angle traversed by a light ray belonging to the photon sphere and its analogue inside the horizon (Sect. 3), the velocity of a uniformly accelerated test particle (Sect. 4) and a generalized Doppler shift (Sect. 5) for the signals exchanged between resting/co-moving observers. In Sects. 6 and 7 we present a Discussion and Final remarks, respectively.

### 2 *t*-observers and *r*-observers

The subject of our considerations will be three distinct spacetimes which confine BHs, Schwarzschild, Reissner–Nordström, and Anti-de Sitter. Outside the horizon they may all be described in terms of a metric in a diagonal form (we will use here the system of units where  $c = G = 1$ ):

$$ds^2 = f dt^2 - f^{-1} dr^2 - r^2 d\Omega^2 \tag{1}$$

where,  $d\Omega^2 = d\theta^2 + \sin^2 \theta d\phi^2$ ,  $\theta, \phi$  denote angular coordinates. Hence for:

(a) the Schwarzschild spacetime

$$f_S(r) = 1 - \frac{r_g}{r} \tag{2}$$

where  $r > r_g = 2M$  and  $r_g$  labels an event horizon (gravitational radius),  $M$  denotes the mass of the black hole.

(b) the Reissner–Nordström spacetime which confines charged black holes with a charge  $Q(\leq M)$

$$f_{RN}(r) = 1 - \frac{2M}{r} + \frac{Q^2}{r^2} \tag{3}$$

$$r_g = r_+, r_{\pm} = M \pm \sqrt{M^2 - Q^2} \tag{4}$$

(c) the Anti-de Sitter spacetime,

$$f_{AdS}(r) = 1 - \frac{2M}{r} + \Lambda r^2 \tag{5}$$

There are four Killing vectors manifesting symmetry properties of a spherically symmetric, static spacetime: a time-like

one and three other space-like ones. In case (1) they are represented by two vectors: a time-like one,  $\partial_t$  reflecting energy conservation due to the static character of the spacetime and a space-like one,  $\partial_\phi$  representing angular momentum conservation.

It was shown explicitly in Ref. [12] but indicated earlier in other sources [13, 14] that despite the singular character of the Schwarzschild metric at the event horizon it may nonetheless be applied also to the interior of the event horizon. Indeed, one can find a solution of Einstein’s equation in the vacuum that is represented by the metric (1) inside the horizon,  $r < r_g$ , i.e.  $f_S(r) < 0$ . The interior of the Schwarzschild BH (see [12]) is a dynamic spacetime where the Killing vector  $\partial_t$  is converted from a temporal into a spatial one. This is accompanied by the interchange of the character of the coordinates:  $t$  becomes spatial and the former radial coordinate  $r$  becomes temporal (see also Ref. [13])

$$ds^2 = \left(-\frac{1}{f}\right) dr^2 - (-f) dt^2 - r^2 d\Omega^2 \tag{6}$$

The spacetime itself becomes homogeneous resulting in a momentum  $t$ -component conservation. A similar interchange of the role of the coordinates  $t$  and  $r$  occurs in AdS spacetime. RN spacetime reveals, apart from the outer event horizon (+) an inner one also, termed a Cauchy horizon (–) (see Eq. 4). In this case the event horizon marks the border between a static (outer) spacetime and a dynamic (inner) one for  $r_- < r < r_+$  with the interchange of the role of the  $t$  and  $r$  coordinates as described above occurring here only between the horizons. Therefore, one can introduce a class of resting observers (or co-moving inside/between the horizon(s) - see below), i.e. those whose velocity vector has only a temporal non-vanishing coordinate. It appears natural to label them as:

(a) *t*-observers

$$U_t^{(i)} = \frac{1}{\sqrt{(f_i)}} \partial_t \tag{7}$$

outside the horizon and

(b) *r*-observers,

$$U_r^{(i)} = -\sqrt{(-f_i)} \partial_r \tag{8}$$

inside the horizon for  $i = S, AdS$  spacetimes or between the outer and inner horizons for  $i = RN$  spacetime.

### 3 Deflection (revolution) angle – a photon sphere and its analogue inside the horizon

Null geodesics are described in terms of a null vector field  $k = k^\mu \partial_\mu$ ,  $k^2 = 0$ . The components of  $k$  are:  $k^\mu = \frac{dx^\mu}{d\sigma}$ ,

where  $x^\mu$  are the coordinates of a given null geodesic and  $\sigma$  denotes an affine parameter. In spherically symmetric spacetimes, geodesics are planar and one can choose an equatorial plane,  $\theta = \frac{\pi}{2}$ , so  $k^\theta = 0$ . Then two of the three non-vanishing components of  $k$  are given by conservation laws:

$$k^t = \frac{\omega_0}{f_i}, k^\phi = \frac{L}{r^2} \tag{9}$$

where  $L$  denotes an angular momentum and outside of the horizon,  $\omega_0$  is interpreted as an energy. The third component is derived from the null condition:

$$k^r = \pm L \sqrt{\frac{1}{b^2} - V_i} \tag{10}$$

where an impact parameter,  $b$ , is defined as  $b = \frac{L}{\omega_0}$ . An effective (“photon”) energy potential

$$V_i(r) = \frac{f_i}{r^2} \tag{11}$$

displays a maximal value at the photon sphere radius (phs). In the case of the Schwarzschild and AdS spacetimes,  $r_{phs} = 3M$  (see Fig. 1).

The critical value of the impact parameter is determined by the maximum of the effective potential energy

$$\frac{1}{b_{cr}^2} = V_i(r_{phs}) \tag{12}$$

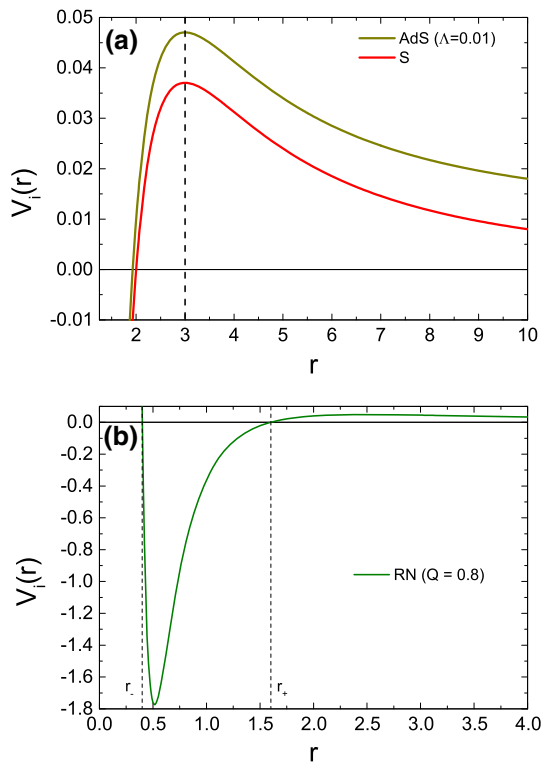


**Fig. 1** An effective energy potential  $V_i(r)$  (Eq. 11) for S, AdS (a) and RN (b) spacetimes ( $M = 1$ )

The wave vector representing the circular orbit belonging to the photon sphere has two non-vanishing components, temporal and angular

$$k = k^t \partial_t + k^\phi \partial_\phi \tag{13}$$

such that,  $b = b_{cr}$ . Though such a circular orbit is unstable the revolution angle, in principle, may be infinite.

In general a light ray specified by an impact parameter  $b$  traverses an angle

$$\Delta\phi_i = \pm \int_{r_1}^{r_2} \frac{dr}{r^2 \sqrt{\frac{1}{b^2} - V_i}} \tag{14}$$

that grows indefinitely when  $b$  tends to its critical value.

Inside (between) the horizon(s),  $f_i < 0$  (and coordinates  $t$  and  $r$  exchange their roles). In this range a null geodesic, characterized by a wave vector with two non-vanishing, “temporal” and angular components (c.f. Eq. 13), has the form:

$$k = k^r \partial_r + k^\phi \partial_\phi \tag{15}$$

It may be regarded as analogous to the photon sphere that occurs outside the horizon. In the case of Schwarzschild spacetime its equation is derived from the null condition for the planar  $\theta = \frac{\pi}{2}$ , trajectory,

$$-f_s(r) = \frac{2M}{r} - 1 \tag{16}$$

$$\omega_0^2 - (k^r)^2 + \left(\frac{2M}{r} - 1\right) r^2 (k^\phi)^2 = 0 \tag{17}$$

and a conserved momentum  $t$ -component condition

$$k_t = \omega_0 = 0 \tag{18}$$

One obtains from Eqs. (17, 18) the expression

$$\Delta\phi_S = \int_{r_1}^{r_2} \frac{dr}{\sqrt{r^2(-f_s)}} \tag{19}$$

for the revolution angle in the case. It is given by the “cardioid” equation:

$$\phi_S = \int \frac{dr}{\sqrt{r(2M-r)}} = \arccos\left(\frac{r}{M} - 1\right) + C. \tag{20}$$

The total revolution angle along the photon sphere-analogue inside the Schwarzschild BH

$$\Delta\phi_S = \int_0^{2M} \frac{dr}{\sqrt{r(2M-r)}} = \pi \tag{21}$$

is equal to  $\pi$ . This result turns out to have a deeper significance.

In the case of RN spacetime by using the same arguments as above, with  $-f_s$  substituted by

$$-f_{RN} = \frac{2M}{r} - 1 - \frac{Q^2}{r^2} \tag{22}$$

between the horizons one obtains the following expression for the revolution angle:

$$\phi_{RN} = \int_{r_-}^{r_+} \frac{dr}{\sqrt{(r_+ - r)(r - r_-)}} \tag{23}$$

Making the substitution,  $x = r - r_-$  one finds that the integral (23) is given as,

$$\Delta\phi_{RN} = \int_0^{r_+ - r_-} \frac{dr}{\sqrt{(r_+ - r_- - x)x}} \tag{24}$$

leading to the total value,

$$\Delta\phi_{RN}^{tot} = \pi \tag{25}$$

the same as in the case of Schwarzschild spacetime.

One can easily confirm that this specific value  $\pi$ , [see Eqs. (21, 24)], is an upper limit for a revolution angle along an arbitrary null geodesic. Indeed, the total revolution angle for the general case of an arbitrary light ray (characterized by  $b^{-1} = \omega_0/L$ )

$$\phi_S^{tot} = \int_{r_1}^{r_2} \frac{\frac{L}{r^2} dr}{\sqrt{(-fs)\frac{L^2}{r^2} + \omega_0^2}} \leq \int_{r_1}^{r_2} \frac{dr}{\sqrt{r^2(-fs)}} \leq \pi \tag{26}$$

turns out to be smaller than  $\pi$  for both Schwarzschild and RN spacetimes (see Fig. 2).

In the case of AdS spacetime the situation is the following. Formula (19) then takes the form:

$$\phi_{AdS}^{tot} = \int_0^{r_g} \frac{dr}{\sqrt{r(2M - r) - \Lambda r^4 + er^4}} \tag{27}$$

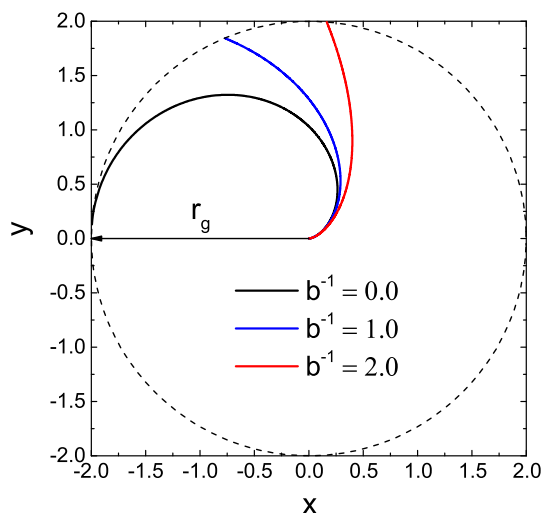


**Fig. 2** Total revolution angle  $\phi_S^{tot}$  (Eq. 26) ( $M = 1$ ), for different values of  $b^{-1}$

and leads to the outcome  $\Delta\phi_{(AdS)}^{tot} < \pi$ . An interesting feature was reported in Ref. [15] where

$$\Delta\phi_{AdS}^{tot} = \int_0^{2M} \frac{dr}{\sqrt{r(2M - r) - \Lambda r^4 + er^4}} \tag{28}$$

integrated from  $r = 2M$  (above the horizon in this case) for  $e = \Lambda$ , yielded the value  $\pi$  (cf. Fig. 1a).

One can ask for the value of the total revolution angle in the case of Kerr spacetime. The situation turns out to be more complex then, but for the case of a light ray in the equatorial plane one can prove that the total revolution angle can't exceed  $\pi$ . In this sense  $\pi$  is an upper limit for the deflection angle of a light ray inside the horizon of an arbitrary black hole.

### 4 Uniform acceleration

In this section we will consider the problem of a test particle uniformly accelerated outside a BH along a radial direction and the analogue of this motion inside the horizon (this Section generalizes the discussion presented in Ref. [9]). Such motion is confined to the  $t$ - $r$  hyperplane:

$$ds^2 = f dt^2 - f^{-1} dr^2. \tag{29}$$

The components of the velocity vector  $u$ ,

$$u = u^t \partial_t + u^r \partial_r \tag{30}$$

of the test particle  $u^t, u^r$  will depend on  $r$ .

An acceleration vector field  $a$  for  $u$  is:

$$a = \nabla_u u \tag{31}$$

and one obtains the following equations for its components

$$a^t = f^{-1} u^r \frac{d}{dr} (f u^r) \tag{32}$$

$$a^r = f u^t \frac{d}{dr} (f u^t) \tag{33}$$

Uniform acceleration is defined by the condition:

$$a^2 = f (a^t)^2 - f^{-1} (a^r)^2 \equiv -\alpha^2 \tag{34}$$

where  $\alpha = \text{const}$ . Formulae (32)–(34) lead to the condition

$$\frac{d}{dr} (f u^t) = \pm \alpha \tag{35}$$

One then finds that Eqs. (32), (33) take on a form similar to the case of uniformly accelerated motion in Minkowski spacetime:

$$a^t = \alpha f^{-1} u^r \tag{36}$$

$$a^r = \alpha f u^t \tag{37}$$

Thus the world line of a uniformly accelerated particle  $\gamma = \{t(\tau), r(\tau)\}$  is given in this case by the integral curve of the

vector field  $u$ :

$$u^t \equiv \dot{t} = \pm \frac{\alpha r + E}{f(r)} \tag{38}$$

$$u^r \equiv \dot{r} = \pm \sqrt{(\alpha r + E)^2 - f(r)} \tag{39}$$

where  $E$  is an integration constant. The components of the velocity vector of the test particle given in general form in Eqs. (38) and (39) are restricted to the following regions:

- (a) outside the horizon,  $\dot{t} > 0$
- (b) inside the horizon,  $\dot{r} < 0$

One easily can find a solution of Eqs. (38) and (39) yielding a world line in this case but such a quantity is coordinate dependent. On the other hand using the velocity vector one can describe this motion in terms of an invariant quantity, the speed of the test particle as measured by a specific (class of) observer(s).

In order to define the speed of a test particle one uses a procedure proposed by Bolos [16]. A velocity four-vector  $w$  of  $u'$  measured by  $u$  at the same event  $p(r, t)$  is given by:

$$w = \frac{u'}{(u, u')} - u \tag{40}$$

where  $(u', u)$  is the scalar product of two velocity four-vectors  $u$  and  $u'$ :  $u^2 = u'^2 = 1$ . Velocity  $w$  is orthogonal to  $u$ ,  $(w, u) = 0$  i.e.  $w$  is a space-like vector as

$$w^2 = \frac{1}{(u, u')^2} - 1 < 0 \tag{41}$$

Then the squared speed  $v^2$  is given by:

$$v^2 = -w^2 \tag{42}$$

#### 4.1 Black hole exterior

Outside the S, RN and AdS black holes the spacetime is static and a resting (static) observer denoted as  $t$ -o is characterized by a velocity vector  $U_t^{(i)}$ , Eq. (7). Such an observer measures the speed  $v$  of a nearby passing uniformly accelerated (ua) test particle,

$$u_{ua} = \dot{t} \partial_t + \dot{r} \partial_r \tag{43}$$

Hence for  $u = U_t^{(i)}$  and  $u' = u_{ua}$ , Eq. 43, due to procedure (40–42) one finds:

$$w^2 = -\frac{\dot{r}^2}{(f\dot{t})^2} \tag{44}$$

Using Eqs. (38), (39) one finds the speed as a function of  $r$

$$v^2 = \frac{(\alpha r + E)^2 - f(r)}{(\alpha r + E)^2} \tag{45}$$

(see Fig. 3).

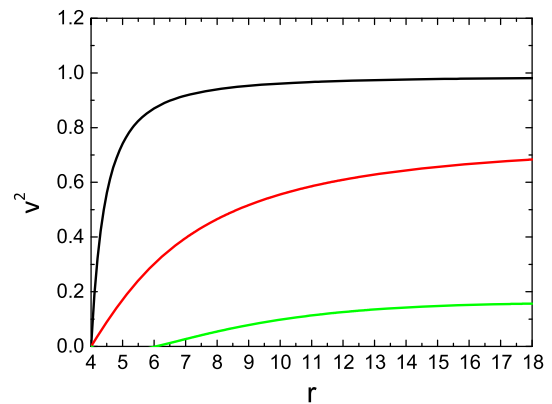


**Fig. 3** (Squared) Speed  $v^2$  (Eq. 45) of a uniformly accelerated particle outside the horizon of the AdS BH for  $\alpha = 1; 0.2; 0.1$  (black/red/green) ( $M = 1, \Lambda = 0.01$ )

#### 4.2 Black hole interior

Inside the horizon of the S, RN and AdS black holes,  $f(r) < 0$  and  $dr < 0$ . The class of resting (co-moving - see below)  $r$ -observers, is determined by their velocity vector (Eq. 8). The squared speed of a uniformly accelerated test particle (38–39) measured by resting observers (8), turns out to be determined as:

$$\bar{v}^2 = \frac{(\alpha r + E')^2}{(\alpha r + E')^2 - f(r)} \tag{46}$$

where  $E'$  is an integration constant. Let us emphasize that the speed outside and inside the horizon are expressed by inverse formulae, Eqs. (45, 46) (see also [8, 9]).

The speed  $\bar{v}^2$  as a function of a temporal coordinate  $r$  may be illustrated in AdS and RN spacetimes (the S case illustrated in Ref. [9], is not much different from the case of AdS spacetime) using (46) (Figs. 4, 5). Analyzing these diagrams one has to remember that in the vicinity of the horizon, either outer or inner,  $f \rightarrow 0$ , and  $\bar{v} \rightarrow 1$ . Hence in S

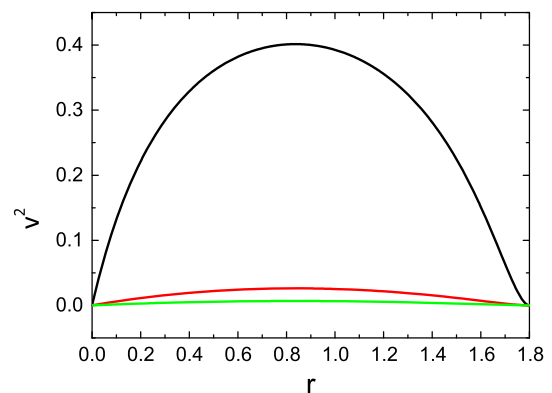


**Fig. 4** (Squared) Speed  $\bar{v}^2$  (Eq. 46) of a uniformly accelerated particle inside the horizon of the AdS BH for  $\alpha = 1; 0.2; 0.1$  (black/red/green) ( $M = 1, \Lambda = 0.01$ )

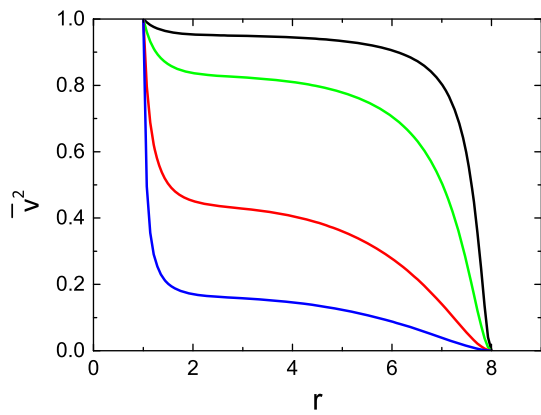


**Fig. 5** (Squared) Speed  $\bar{v}^2$  (Eq. 46) of a uniformly accelerated particle inside the horizon of the RN BH for  $\alpha = 1; 0.5; 0.2; 0.1$  (black/green/red/blue) ( $M = 5, Q = 3$ )

and AdS spacetimes, the speed of the initially resting particle increases, reaches some (non-universal) maximal value and decreases to zero at the ultimate singularity,  $r \rightarrow 0$  (Fig. 4).

In the case of RN, initially  $\bar{v}^2$  increases then it may behave in a mixed manner and finally it tends to the value 1 at the internal horizon.

### 5 Exchange of electromagnetic signals

In this section we shall consider the case of two resting observers (static outside and co-moving inside the horizon),  $A$ , and  $B$ , exchanging electromagnetic signals. Without loss of generality one can assume that  $A$  and  $B$  are restricted to the equatorial plane,  $\theta = \frac{\pi}{2}$ . Then the generalized Doppler shift, i.e. the frequency ratio of the receiver (r) and sender (s) is expressed as:

$$\frac{\omega^{(r)}}{\omega^{(s)}} = \frac{u^{(r)} \cdot k^{(r)}}{u^{(s)} \cdot k^{(s)}} \tag{47}$$

where  $u^{(r/s)} \cdot k^{(r/s)}$  denotes the scalar product of the receiver/sender velocity vector and the wave vector at the receiver/sender position. Applying the fact that outside and inside the horizon resting observers are  $t$ -observers and  $r$ -observers, respectively, and using the following form for the wave vector

$$k = \frac{\omega_0}{f} \partial_t \pm \sqrt{\omega_0^2 - f \frac{L^2}{r^2}} \partial_r - \frac{L}{r^2} \partial_\phi \tag{48}$$

one obtains the following results.

#### 5.1 Outside the horizon

If  $A, B$  are placed at  $(r_A, \frac{\pi}{2}, \phi_A), (r_B, \frac{\pi}{2}, \phi_B)$  respectively,  $r_g < r_A < r_B$  then,

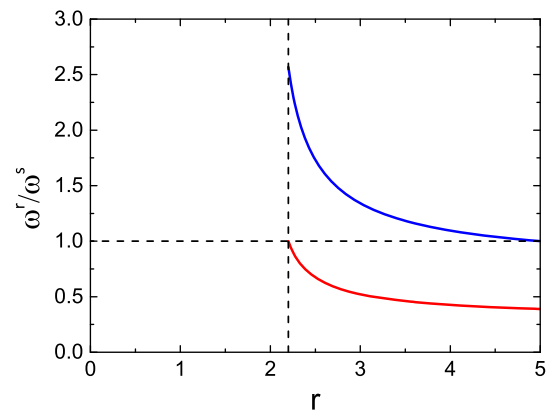


**Fig. 6** Frequency shift outside the horizon of a Schwarzschild BH: signals exchanged between  $A$  and  $B$ ,  $A-B$  (gravitational redshift) and  $B-A$  (gravitational blueshift),  $r_A = 2.2, r_B = 5; (M = 1)$

(a)  $A$  (r-receiver) records the signal sent by  $B$  (s-sender)

$$\frac{\omega_A^r}{\omega_B^s} = \frac{\sqrt{f(r_B)}}{\sqrt{f(r_A)}} > 1 \tag{49}$$

as blue-shifted and

(b)  $B$  (r) records the signal sent by  $A$  (s)

$$\frac{\omega_B^r}{\omega_A^s} = \frac{\sqrt{f(r_A)}}{\sqrt{f(r_B)}} < 1 \tag{50}$$

as red shifted which is a well-known result (see Fig. 6).

#### 5.2 Inside the horizon

If  $A, B$  are placed at  $(t_A, \frac{\pi}{2}, \phi_A), (t_B, \frac{\pi}{2}, \phi_B), r_B < r_A$ , respectively, then sending and receiving signals they would find the Doppler shift as follows:

$$\frac{\omega_B^r}{\omega_A^s} = \frac{\sqrt{-f(r_A)} \sqrt{\omega_0^2 - f(r_B) \frac{L^2}{r_B^2}}}{\sqrt{-f(r_B)} \sqrt{\omega_0^2 - f(r_A) \frac{L^2}{r_A^2}}} \tag{51}$$

Transforming expression (51)

$$\frac{\omega_B^r}{\omega_A^s} = \frac{\sqrt{-\frac{\omega_0^2}{f(r_B)} + \frac{L^2}{r_B^2}}}{\sqrt{-\frac{\omega_0^2}{f(r_A)} + \frac{L^2}{r_A^2}}} \tag{52}$$

one finds an interesting outcome. The second term inside the square root increases as  $r$  decreases; for decreasing  $r$  the first term decreases for S and AdS spacetimes and it is a non-monotonic function of  $r$  for RN spacetime. One can consider then two separate cases.



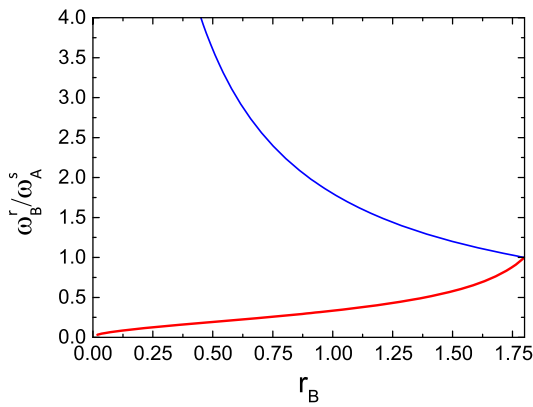


**Fig. 7** Frequency shift inside the horizon of a Schwarzschild BH: signals propagating along the homogeneity ( $t$ ) axis, Eq. (54) are redshifted (red) and signals propagating perpendicularly to the  $t$ -axis (57) are blueshifted (blue); ( $M = 1$ ),  $r_A = 1.75$

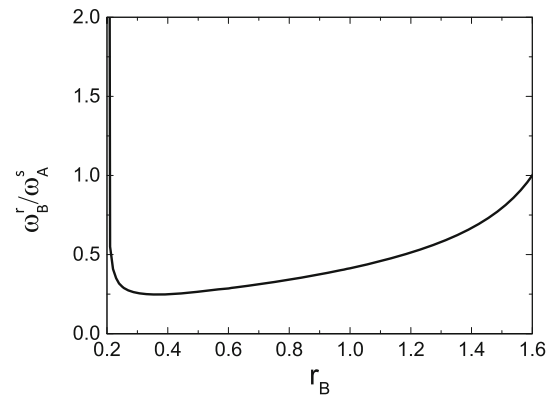


**Fig. 8** Frequency shift inside horizon of RN BH ( $M = 1$ ,  $Q = 0.6$ ), for signals propagating along the  $t$ -axis  $r_- = 0.2 < r_B < r_A = 1.6$ : initial redshift Eq. (55) is followed by the final blueshift Eq. (56) (due to expansion followed by contraction)

5.2.1  $L = 0$  - signals exchanged along the  $t$ -axis

$B$  (receiver) records the signal sent by  $A$  (sender),  $r_B < r_A$  as [see Eq. (52)]

$$\frac{\omega_B^r}{\omega_A^s} = \frac{\sqrt{-f(r_A)}}{\sqrt{-f(r_B)}} \tag{53}$$

This expression leads to different results in S, AdS and RN spacetimes.

In the case of S and AdS black holes  $f(r)$  is a monotonic function of  $r$  and (53) describes a Doppler *redshift* (see Fig. 7)

$$\frac{\omega_B^r}{\omega_A^s} < 1 \tag{54}$$

In the case of a RN black hole one finds mixed results: a Doppler *redshift*,

$$\frac{\omega_B^r}{\omega_A^s} < 1 \tag{55}$$

for  $r_m < r_B < r_A$ , and a Doppler *blueshift*

$$\frac{\omega_B^r}{\omega_A^s} > 1 \tag{56}$$

(see Fig. 8) for  $r_B < r_m = \frac{Q^2}{M}$  where  $f_{RN}(r_m) = \min f_{RN}(r)$ .

5.2.2  $\omega = 0$  - signals exchanged perpendicularly to the  $t$ -axis

If the signal is sent perpendicularly to the  $t$ -direction,  $\omega_0 = 0$ , then, it travels between  $\phi_A$  and  $\phi_B$ . It is emitted at  $r_A$ , recorded at  $r_B$  and by using (52) one finds:

$$\frac{\omega_B^r}{\omega_A^s} = \frac{r_A}{r_B} > 1 \tag{57}$$

A Doppler blueshift is found in all three cases, for S, AdS and RN spacetimes (see Fig. 7). This represents a contraction of this cosmology perpendicular to the direction of homogeneity.

6 Discussion

The discussion above used a coordinate system that was a natural choice for the region outside the horizon. It is a rather widely accepted fact that despite its pathological character at the BH horizon,  $r = r_g$  this coordinate system may also be applied inside the horizon and in the case of Schwarzschild spacetime this has been proven by Doran et al. [12]. The description provided by Eqs. (1) and (6) is not unique and there exist a variety of singularity-free coordinate systems. It is of interest therefore to identify which results in this paper are coordinate independent and which parts of the discussion do depend on the frame of reference used. Hence we will briefly discuss the treatment of some of the problems discussed above in terms of selected singularity-free coordinate systems. We have already shown that Kruskal-Szekeres coordinates applied to the generalized Doppler frequency shift yield the same results as those obtained in Schwarzschild coordinates [8]. On the other hand, a very interesting approach, especially with regard to the main issue of the current paper, is presented within a so-called “river model” based on the use of Gullstrand–Painlevé (G–P) coordinates within Schwarzschild space-time (2) (see [6, 17]). In the G–P metric, the  $t$ -coordinate is substituted with the proper time  $\tilde{t}$  of a  $v$ -observer.

$$u_v = \frac{1}{1 - v^2} \partial_{\tilde{t}} - v \partial_t \tag{58}$$

freely falling from infinity, where the parameter  $v = \sqrt{\frac{2M}{r}}$  is regarded as a “velocity of space” (Refs. [6, 17]), such that at the horizon  $v = 1$  and inside the horizon  $v > 1$ ,

$$d\tilde{t} = dt + \frac{v}{1 - v^2} dr. \tag{59}$$

Hence the transformation between Schwarzschild  $t, r$  and G-P,  $\tilde{t}, R$  coordinates is given by

$$\frac{\partial(\tilde{t}, R)}{\partial(t, r)} = \begin{bmatrix} 1 & \frac{v}{1-v^2} \\ 0 & 1 \end{bmatrix}. \tag{60}$$

By using an appropriate tetrad for a  $v$ -observer, one can describe, from the perspective of such a co-moving observer, a variety of processes or phenomena (e.g. the Penrose mechanism inside a BH – see [17]). A test object is described by a  $v$ -observer in terms of the velocity vector, “peculiar velocity”  $v_p$ , expressed using this tetrad basis set. One can then ask for the velocity of a uniformly accelerated test particle, as in Sect. 4, as perceived by the  $v$ -observer. Before doing this let us consider the perception by a co-moving observer of three specific test objects: a resting  $t$ -object ( $t$ - $o$ ) (7), an  $r$ -observer (8), ( $r$ - $o$ ) “resting” inside the horizon and a freely falling test object,  $\varepsilon$ - $o$

$$U_{\varepsilon-o} = \frac{\varepsilon}{1 - v^2} \partial_t - \sqrt{\varepsilon^2 - 1 + v^2} \partial_r. \tag{61}$$

The velocity vectors of these three test objects in the local frame of a co-moving observer, i.e. projections on the tetrad vectors, allow the determination of the peculiar velocity. This may be done according the prescription given by Toporensky and Zaslavskii [17] (see also [6]). On the other hand, if one is interested in the value of peculiar velocity then one can simplify this task to determining only the respective speed, and this value of  $v_p$  is determined by the scalar product,

$$u_v U_o = \frac{1}{\sqrt{1 - v_p^2}} \tag{62}$$

Accordingly, for these three objects one obtains the following values for the squared peculiar velocity: for the  $t$ - $o$

$$v_p^2(t - o) = v^2, \tag{63}$$

for the  $r$ - $o$

$$\tilde{v}_p^2(r - o) = \frac{1}{v^2}, \tag{64}$$

and for  $\varepsilon$ - $o$

$$v_p^2(\varepsilon - o) = 1 - (u_v U_\varepsilon)^{-2} \tag{65}$$

where,

$$u_v U_\varepsilon = \frac{\varepsilon^2 + v^2}{\varepsilon + v\sqrt{\varepsilon^2 - 1 + v^2}}. \tag{66}$$

Expressions (63) and (64) coincide with the conclusions (and the results) of paper [8] [cf. also Eqs. (45), (46)]. Expression

(65) has two notable properties: on the horizon,  $v = 1$ , it takes a value smaller than 1

$$v_p^2(\varepsilon - o) = \left( \frac{\varepsilon^2 - 1}{\varepsilon^2 + 1} \right)^2 \tag{67}$$

and at the ultimate singularity,  $r \rightarrow 0$ , it vanishes

$$v_p^2(\varepsilon - o) \rightarrow 0 \tag{68}$$

For the squared peculiar velocity (65) expressed in terms of  $v$ , and  $V = \frac{\sqrt{\varepsilon^2 - 1 + v^2}}{\varepsilon}$ , the speed of  $\varepsilon$ - $o$  with respect to a static observer,  $t$ - $o$  (7), one gets,

$$v_p^2(\varepsilon - o) = \left( \frac{v - V}{1 - vV} \right)^2 \tag{69}$$

i.e. the result given by Toporensky and Zaslavskii [17] as Eq. (33). Let us present now the case of a uniformly accelerated ( $ua$ - $o$ ) test particle (Sect. 4) as perceived by a co-moving observer (58). The components of the peculiar velocity may be determined in the tetrad of the  $v$ -observer (see [17]), but as underlined above the squared value of this quantity,  $v_p^2(ua-o)$  is simply given as

$$v_p^2(ua - o) = 1 - (u_v U_{ua})^{-2} = \frac{A}{A + g_{tt}^2} \tag{70}$$

where

$$A = 2(\alpha r + E')[(\alpha r + E') + v\sqrt{(\alpha r + E')^2 - g_{tt}}] - g_{tt}[1 + (\alpha r + E')^2]. \tag{71}$$

Two interesting results following from Eq. (70) for the squared velocity of a uniformly accelerated test particle with respect to a co-moving observer are the initial and final values. As the initial speed with respect to a resting,  $r$ -observer observer is zero,  $(\alpha r + E') = 0$ , the initial speed as perceived by a  $v$ -observer obtained from (70) is:

$$\tilde{v}_p^2(ua - o) = \frac{1}{v^2}. \tag{72}$$

At the ultimate singularity  $r \rightarrow 0$  and  $g_{tt}^2 \rightarrow \infty$ , the (squared) peculiar velocity tends, as is known, to zero,

$$\tilde{v}_p^2(ua - o) = \frac{1}{g_{tt}} \rightarrow 0. \tag{73}$$

The latter result, Eq. (73), complies with the outcome about expansion at the ultimate singularity. The former one (Eq. (72)), complies with expectations: a test particle is initially at rest with respect to a resting observer,  $r$ - $o$  so its squared speed with respect to the  $v$ -observer, Eq. (72), is the same as the squared speed of the  $r$ - $o$  observer Eq. (64) One may conclude these considerations as follows. Utilising coordinate frames free of singularities one obtains a coherent tool for describing processes taking place above and inside the horizon, and  $t, r$  coordinates are pathological on the horizon



Nevertheless it is more natural to apply  $t, r$  coordinates outside and inside the horizon bearing in mind the interchange of their roles, as it is a natural frame of reference and a useful perspective for identifying analogies and illustrations as was done in Secs. 3-5. It should be underlined that when we are looking for invariant quantities and expressions that are represented in terms of invariant objects such as scalar products, then all of the frames of reference mentioned above that are regular at the horizon, such as the Gullstrand-Painlevee, Kruskal-Szekeres or other systems, and Schwarzschild coordinates - albeit ill-defined at the horizon - end up leading to the same outcomes as already discussed. Then the matter of choice of coordinate system depends on the context of the issues to be discussed. This may result in different perspectives - such as the “river model” approach - along with a static, isotropic system outside the horizon but an anisotropic, dynamic system inside the horizon of a Schwarzschild black hole.

### 7 Final remarks

The aim of this paper was to present the properties of the interior of BHs for spherically symmetric spacetimes. We have discussed three specific effects: an angle traversed by a light ray on a photon sphere, the speed of a uniformly accelerated test particle and the generalized Doppler effect i.e. the frequency shift for electromagnetic signals exchanged between resting (or co-moving) observers. We compared the results obtained for the exterior and interior of the BHs. In this way we have illustrated (selected) properties of the interior (and also the exterior) of an event horizon of these classes of black holes.

The main outcomes are as follows. Inside the horizon of a BH one can find an analogue of the photon sphere. In fact this turns out to be a sphere with an ever decreasing radius, from  $r_g$  to 0 for S and AdS black holes or from  $r_+$  to  $r_-$ , for an RN black hole. The total revolution angle of a light ray belonging to such a “photon sphere” is  $\pi$  for the Schwarzschild and Reissner–Nordström spacetimes; it is smaller than  $\pi$  in the case of Anti-de Sitter spacetime. It should be emphasized that the angle traversed by a light ray on the photon sphere outside the horizon is, in principle, infinite. There is a finite lifetime within the horizon, so it isn’t bizarre that the angle swept out by a ray belonging to a photon sphere analogue turns out to be finite. It is interesting that it takes the value  $\pi$  and the fact that for Kerr black holes this value also appears to be an upper limit. Although no physical argument for this result has yet been found, an intriguing correspondence might be indicated. An important issue from a recent idea, referred to by its author G. ’tHooft as “new physics” [18], is “antipodal identification” (see also [19]). Antipodal identification means

in fact that there is a symmetry relation  $\phi \rightarrow \phi + \pi$  inside the horizon.

But this is actually the meaning of our result. Therefore, so as not to contradict the idea of antipodal identification, the total traversed angle could not exceed  $\pi$ .

A uniformly radially accelerated test particle outside the horizon satisfies the generalized equations of those known from Minkowski spacetime and behaves in a more or less understandable manner. During its inward motion, the particle accelerates, i.e. its speed increases as the particle approaches the event horizon:

$$v^2 = \frac{(\alpha r + E)^2 - f(r)}{(\alpha r + E)^2} \rightarrow 1 \tag{74}$$

The fact that the value of the speed tends to 1 ( $v \rightarrow c$ ) is a property of the horizon,  $f(r) = 0$ . In the case of outward motion, the particle starting at  $r_0$  can move outward only if its acceleration is larger than some critical value  $\alpha_{cr}(r_0)$ ; otherwise the particle will move inward. The critical acceleration

$$\alpha_{cr}(r_0) = \frac{1}{f(r_0)} \frac{r_g}{r_0^2} \tag{75}$$

turns out to be equal to the gravitational acceleration of an object resting at  $r_0$ . In the case of outward motion from rest,  $r = r_0, \alpha > \alpha_{cr}(r_0)$  the particle goes to infinity and the well-known Rindler frame may be observed asymptotically. In this sense the test particle behaves in an understandable manner.

In the case of Schwarzschild spacetime, inside the horizon the speed is given by an expression inverse to the one above the horizon. As underlined elsewhere [8] it is a manifestation of the interchange of the roles of  $t$  and  $r$  coordinates. This is the case in AdS and RN spacetimes as well, though in RN spacetime it takes place between horizons.

The speed of a test particle uniformly accelerated along the homogeneous  $t$ -axis inside the horizon of a Schwarzschild BH initially increases but after reaching a (non-universal) maximal value decreases asymptotically to zero at the ultimate singularity (see also [9]). Similar behavior may also be observed within an AdS black hole. In the case of RN spacetime, where an inner, Cauchy horizon is developed, the speed of a uniformly accelerated test particle behaves in a mixed manner. Initially growing, it may decrease at some stage, eventually tending to 1 at the inner horizon. However unexpected this observation may seem, the speed of the test particle inside the S and AdS horizons on the one hand and between the RN horizons, on the other, it turns out to be coherent with a specific feature of these media. It becomes clearer after analysing the generalized Doppler effect, i.e. frequency shift.

The exchange of electromagnetic signals, between observers resting outside an event horizon leads to the well-known gravitational Doppler red- or blueshift. We have

shown that inside the horizon signals propagating along the homogeneous  $t$ -axis are redshifted in S and AdS black holes. But they are initially redshifted and finally blueshifted inside RN black holes. This means that the interior of S and AdS black holes expand along the  $t$ -direction and the accompanying effect is a “cosmological-like” Doppler redshift (see also [12]). That expansion affects both “resting”, (in this case “co-moving”) and travelling (e.g. a uniformly accelerated test particle) objects in such a manner that their mutual motions vanish when approaching the ultimate singularity (see also [20]). A uniformly accelerated particle turns out to finally slow down (asymptotically) to zero.

The interior of an RN black hole on the other hand may be viewed as initially,  $r_+ > r > r_m$  expanding until  $r = r_m$ ,

$$f'_{RN}(r_m) = 0 \quad (76)$$

and finally,  $r_m < r < r_-$  becoming a contracting spacetime. This is accompanied by an appropriate “cosmological” Doppler frequency shift, redshift first followed by the final blueshift. In this case a uniformly accelerated test particle may at some stage “slow down” (this is an acceleration value dependent result), but then, due to contraction along the  $t$  direction rather than due to acceleration, its speed increases to 1 when approaching the inner horizon,  $f(r_-) = 0$ . Such a conclusion is confirmed by calculating the behaviour of a freely falling test particle [8], whose varying speed simply “mimics” the variations in  $f_i(r)$  in the black hole’s interior.

Let us emphasize an asymmetry of the evolution of the interior of spherically symmetric (outside the horizon) Schwarzschild, Anti-de Sitter and Reissner–Nordstrom spacetimes. Signals propagating perpendicularly to the  $t$ -axis are found to be blueshifted confirming the result found for Schwarzschild spacetime in [9]. One may guess that such a contraction should affect specific time-like world lines. In fact, this kind of effect may be observed (details will be presented elsewhere). For an accelerated particle whose trajectories belong to the photon sphere analogue in the interior of S and AdS black holes its speed (as measured by resting observers) grows to 1, independently of the value of acceleration, when approaching the ultimate singularity,  $r \rightarrow 0$ ; in the case of an RN black hole interior, the value of the speed of an accelerated particle tends to a value smaller than 1 however as  $r \rightarrow r_-$ .

We have described then how (some) non-quantum processes would be dramatically affected by the dynamics of the black holes interior. Even more interesting is the question of how the dynamically changing spacetime of the interior of black holes would affect quantum processes. That will be the subject of our further studies.

**Data Availability Statement** This manuscript has no associated data or the data will not be deposited. [Authors’ comment: There is no accompanying data to present. The paper is theoretical/modelling research, and all relevant data are presented graphically in the paper itself.]

**Open Access** This article is distributed under the terms of the Creative Commons Attribution 4.0 International License (<http://creativecommons.org/licenses/by/4.0/>), which permits unrestricted use, distribution, and reproduction in any medium, provided you give appropriate credit to the original author(s) and the source, provide a link to the Creative Commons license, and indicate if changes were made. Funded by SCOAP<sup>3</sup>.

## References

1. A. Almheiri, D. Marolf, J. Polchinski, J. Sully, Black holes: complementarity or firewalls? *J. High Energy Phys.* **2013**(2), 1–19 (2013)
2. S.W. Hawking, M.J. Perry, A. Strominger, Soft Hair on Black Holes. *Phys. Rev. Lett.* **116**(23), 231301 (2016)
3. M. Christodoulou, C. Rovelli, How big is a black hole? *Phys. Rev. D Part Fields Gravit. Cosmol.* **91**(6), 064046 (2015)
4. P. Gusin, A. Radosz, The volume of the black holes—the constant curvature slicing of the spherically symmetric spacetime. *Modern Phys. Lett. A* **32**(22), 1750115 (2017)
5. S.L. Braunstein, S. Pirandola, K. Zyczkowski, Better late than never: Information retrieval from black holes. *Phys. Rev. Lett.* **110**(10), 13–17 (2013)
6. A.J.S. Hamilton, J.P. Lisle, The river model of black holes. *Am. J. Phys.* **76**, 519 (2004)
7. W.G. Unruh, Experimental Black-Hole Evaporation? *Phys. Rev. Lett.* **46**(21), 1351–1353 (1981)
8. A.T. Augousti, P. Gusin, B. Kuśmierz, J. Masajada, A. Radosz, On the speed of a test particle inside the Schwarzschild event horizon and other kinds of black holes. *Gen. Relativ. Gravit.* **50**(10), 131 (2018)
9. P. Gusin, A. Augousti, F. Formalik, A. Radosz, The (A)symmetry between the Exterior and Interior of a Schwarzschild Black Hole. *Symmetry* **10**(9), 366 (2018)
10. A.J. Hamilton, G. Polhemus, Stereoscopic visualization in curved spacetime: Seeing deep inside a black hole. *New J. Phys.* **12**, 123027 (2010)
11. A.V. Toporensky, O.B. Zaslavskii, Redshift of a photon emitted along the black hole horizon. *Eur. Phys. J. C* **77**(3), 179 (2017)
12. R. Doran, F.S. Lobo, P. Crawford, Interior of a Schwarzschild black hole revisited. *Found. Phys.* **38**(2), 160–187 (2008)
13. V.P. Frolov, I.D. Novikov, *Black Hole Physics: Basic Concepts and New Developments* (Kluwer Academic, Dordrecht, 1998)
14. S.W. Hawking, G.F.R. Ellis, *The Large Scale Structure of Space-Time* (Cambridge Univ Press, Cambridge, 1973)
15. N. Cruz, M. Olivares, J.R. Villanueva, The geodesic structure of the Schwarzschild anti-de Sitter black hole. *Class. Quantum Gravity* **22**(6), 1167–1190 (2005)
16. V.J. Bolós, Intrinsic definitions of “relative velocity” in general relativity. *Commun. Math. Phys.* **273**(1), 217–236 (2007)
17. A.V. Toporensky, O.B. Zaslavskii, Zero-momentum trajectories inside a black hole and high energy particle collisions. [arXiv:1808.05254](https://arxiv.org/abs/1808.05254), (2019)
18. G. ’t Hooft, The Firewall Transformation for Black Holes and Some of Its Implications. *Found. Phys.* **47**(12), 1503–1542 (2017)
19. N. Sanchez, B.F. Whiting, Quantum field theory and the antipodal identification of black-holes. *Nuclear Phys. Sect. B* **283**(C), 605–623 (1987)
20. A.V. Toporensky, O.B. Zaslavskii, S.B. Popov, Unified approach to redshift in cosmological/black hole spacetimes and synchronous frame. *Eur. J. Phys.* **39**(1), 015601 (2018)